Radiation and divergence times of Batoidea

EDUARDO VILLALOBOS-SEGURA[*,1] and CHARLIE J. UNDERWOOD[1]

[1]School of Earth Sciences, Birkbeck College, Malet Street, London WC1E 7HX, U.K. elasmo177@gmail.com; c.underwood@bbk.ac.uk.

*Corresponding author

Eduardo Villalobos-Segura; elasmo177@gmail.com

Running head

Villalobos-Segura and Underwood – Radiation and divergence times of Batoidea

ABSTRACT— We present a time-scaled analysis based on morphological characters to estimate the divergence ages for the major batoids clades. Two approaches were used: Tip-dating, which allows the extinct taxa to be included as terminals, assessing the phylogenetic relations and their divergence time simultaneously; and basic and minimum branch length ("a posteriori" methods) that date a pre-existing unscaled topology, given a set of stratigraphic data for the taxa involved. We used stratigraphic indexes to compare the divergence ages recovered by both methods. The tip-dating approach obtained a more resolved topology and slightly better stratigraphic indexes scores than the other methods. Overall the tip-dating analysis recovered slightly earlier divergence ages than the rest of the time dating analyses and the known fossil record of the groups. However, these divergence ages were not as old as those estimated by molecular analysis. Our results suggest the diversity increase through the Late Jurassic-Early Cretaceous might not be gradual, and that Early Cretaceous diversity could be significantly higher. As several divergence events are placed in the Early Cretaceous, there is a suggestion that an active period of cladogenesis leads to the Late Cretaceous high diversity. The last divergence events recovered by the present analysis occurred in the Paleogene and led to the extant groups of batoids.

INTRODUCTION

Phylogenetic comparative methods are a powerful tool for understanding biological evolution. These methods reach an even greater potential when they are scaled through time, allowing the estimation of divergence times and node ages (Bapst & Hopkins, 2017). This estimation is achieved by combining a set of fossil calibrations that constrain the minimum age of the nodes and a phylogenetic analysis or a phylogeny that includes those taxa (Lloyd et al., 2016).

There are two main approaches for time-scaling a phylogeny: Tip-dating and *a posteriori* time-scaling (APT). Tip-dating simultaneously infers both relationships and divergence dates for a set of taxa, whereas APT methods date a pre-existing unscaled topology, given a set of stratigraphic data for the taxa involved (Lloyd et al., 2016; Bapst et al., 2016).

Tip-dating is a relatively new approach, commonly implemented by Bayesian phylogenetic software such as Mr Bayes or BEAST 2 for the analysis of molecular data (Bapst & Hopkins, 2017). This approach uses fossils as priors to estimate maximum and minimum divergence times that give temporality to the branch lengths (i.e., changes between terminals). It differentiates from other model-based analyzes in that it looks for a set of nodal depths (i.e., the distance between an ancestral node to its descendants) that maximizes the probability of obtaining the data set. This method not only recovers the evolutionary events within a group but also estimates the magnitude and rates of changes within and among them, allowing the identification of critical evolutionary events (Benton & Donoghue, 2007). The tip-dating approach requires character and stratigraphic data to generate a probability model that describes the expected waiting times between branching events and a clock model that makes assumptions on the rates of character changes across the tree. The clock model can be strict (i.e., when rates of characters state changes are the same across the tree), or relaxed (i.e., when variation in the rates of character state changes across branches) (Stadler, 2010; Baum & Smith, 2013; Stadler & Yang, 2013).

A posteriori time-scaling methods work independently of the phylogenetic analysis and rely solely on occurrence data (i.e., first and last age appearance). Most APT approaches involve simple algorithms that often translate in incongruence between the phylogeny and the order of stratigraphic appearance, creating zero-length branches (ZLB) (polytomies). For trait evolution,

this is problematic, as any evolutionary changes across ZLB will appear as instantaneous (Bapst, 2013). Several successive APT methods have been developed to avoid the methodological issues of ZLB, (e.g., minimum length branches and equal branch length). These approaches suffer from arbitrary choices of required variables, make strong assumptions on the quality of the fossil record without reference to that fossil record (Lloyd, 2016) and do not allow uncertainties in node ages (Bapst, 2013).

Batoids are the most diverse group of Neoselachii (i.e., modern-type sharks and rays) (sensu Compagno, 1977), with approximately 665 extant species (Fricke et al., 2019). Phylogenetically, they are considered a monophyletic group in a sister relationship to sharks (Dunn & Morrissey, 1995; Schwartz & Maddock, 2002; Douady et al., 2003; Winchell et al., 2004; Aschliman et al., 2012a; b; Naylor et al., 2012; Last et al., 2016). The earliest unambiguous fossil remains of the group come from the Early Jurassic (Toarcian) (Cappetta, 2012). However, a Late Triassic-Early Jurassic origin for the group has been suggested by molecular analysis (e.g., Aschliman et al., 2012b), although no unequivocal Triassic remains have been found. It is hypothesized that some neoselachian remains from the Late Triassic (e.g., †*Doratodus*, †*Vallisia* and †*Pseudodalatias*) could be early representatives of batoids (Cuny & Benton, 1999; Botella et al., 2009). Aschliman et al. (2012b) Triassic estimation of the origin of batoids could be the result of using †"*Dasyatis*" *speetonensis* Underwood et al., 1999 as the calibration lineage for the analysis. A calibration lineage is that with the longest proportion of its true temporal range captured by the fossil record and the age of the oldest fossil of this lineage provides the best minimum age constraint for the calibration of the phylogeny (Marshall, 2008). If †"*D.*" *speetonensis* is considered a myliobatiform, it will extend by 30 million years (Ma) the known age of the group, leaping from the Cenomanian (possible Albian) to the Hauteruvian. Being the

analysis calibration lineage, this will subsequentially move forward the ages of all the remaining clades.

†"*D.*" *speetonensis* was not included in the present analysis, as it is only known from tooth remains, that will not provide grouping information as a terminal for the analysis of a matrix mostly based on skeletal characters, but also due to the taxonomic uncertainties associated with this species, which is unlikely to be a crown dasyatid and might be a hexatrygonid (Cappetta, 2012).

Fossil batoids remain an overlooked group, mostly studied as part of a more extensive analysis of the Neoselachii despite the substantial ecological differences between them and sharks. Diversity estimation analyses for Neoselachii suggest episodic events of diversification events through the Jurassic, Cretaceous, and Palaeocene (Kriwet & Benton, 2004; Underwood, 2006; Guinot et al., 2012a).

Based on Villalobos et al. (2019a) phylogenetic analysis, the current study presents an estimated divergence time for batoids. The analysis includes four sclerorhynchoid genera (†*Sclerorhynchus*, †*Libanopristis*, †*Ptychotrygon*, and †*Asflapristis*) known from almost complete fossil remains. Sclerorhynchoids are an important and probably the best-known extinct clade of Cretaceous batoids. However, their affinities and their position within the batoid radiation are uncertain. Along with these sclerorhynchoid taxa, several Jurassic and Cretaceous species and fossil representatives of all modern batoid clades were included in the analysis, making it the first time-scaled phylogenetic analysis using morphological characters for batoids. The phylogenetic analysis includes topological constrains to account for the phylogenetic relations recovered for the fossil taxa by previous works (De Carvalho, 2004; Naylor et al., 2012; Claeson et al., 2013; Brito et al., 2013;2019; Last et al., 2016; Underwood & Claeson, 2017; Villalobos et al., 2019a); and

the designation of major extant taxonomic groups (orders) (Naylor et al., 2012; Last et al., 2016; Fricke et al., 2019).

Both time-scaling methods (tip-dating and APT) were used and compared with each other by using stratigraphic consistency indexes (Sansom et al., 2018). Ultimately the divergence ages of the method with the best stratigraphic consistency scores were contrasted against previous diversity analyses (e.g., Kriwet & Benton, 2004; Underwood, 2006; Guinot et al., 2012a).

MATERIAL AND METHODS

Institutional abbreviations—AMNH, American Museum of Natural History. BHN, Muséum d'Histoire Naturelle de Boulogne-Sur-Mer. BRC, Birkbeck Reference Collection. BSP, Bayerishe Staatssammling fur Paläontologie und Geologie, Munich, Germany. CNPE-IBUNAM, National Collection of Fishes, Biology Institute, Universidad Nacional Autónoma de México (UNAM). JM-SOS, Jura Museum Eichtätt, Germany. MNHN, Muséum national d'Histoire naturelle, Paris. NHMUK, Natural History Museum United Kingdom, London. UERJ, Universidade do Estado do Rio de Janeiro.

Material examined

Fossil material examined—†*Asflapristis cristadentis*, NHMUK PV P 73925, 75428 a-e, 75429 a-d, 75431, 75432, 75433). †*Asterodermus platypterus*, NHMUK P12067, 10934; JM-SOS 3647. †*Asterotrygon maloneyi*, AMNH P 11557 FMNH PF 12914, 12989, 12990, 14069, 14097, 14098, 14567, 15166, 15180; Specimens figured in de Carvalho (2004; text-figs. 1-13). †*Belemnobatis morinicus*, BHN 2P1. †*Britobatos primarmatus*, MNHN 1946.18.94; NHMUK PV P 4015, 4016, 49517. †*Cyclobatis major*, NHMUK P 4010, 4011, 49514 63175. †*Cyclobatis*

radians, NHMUK P 61243. †*Cyclobatis tuberculatos,* NHMUK PV P 10436. †*Cyclobatis oligodactylus,* NHMUK PV P 601. *"†Dasyatis" zignii,* MGP-PD 150Z/151Z; Specimen figured in Marramà et al. (2018; text-fig: 8). †*Iansan beurleni,* DGM-917, 918, NHMUK P62947(1). †*Kimmerobatis etchesi,* K874, K1894. †*Libanopristis hiram,* NHMUK PV P 108705, 108706, 13858, 63610, 75075. †*Heliobatis radians* AMNH P 19665, FMNH PF 2020. Specimens figured in de Carvalho (2004; text-figs. 28-29). †*Promyliobatis gazolae* MCSNV VII.B.90. †*Ptychotrygon rostrispatula,* NHMUK PV P73630, 75496, 75497, 75498, 75500. †*Raja davisi,* NHMUK PV P 4780, FMNH UF 295. †*"Rhinobatos" tenuirostris,* NHMUK 4770. †*"Rhinobatos" maronita,* MNHN 1946.17.274, NHMUK P4012, 48215, 10696, 39233, 49511. †*"Rhinobatos" latus,* NHMUK PV P4014. †"*Rhinobatos" intermedius,* NHMUK PV P49516, MNHN-SHA-1643. †*"Rhinobatos" grandis,* NHMUK PV P 4013, 49513, 13861. †"*Rhinobatos" whitfieldi,* NHMUK P 9145, 63187, 63199, 24965. †"*Rhinobatos" hakelensis,* MNHN 1946-17-272. †"*Rhinobatos" latus,* NHMUK PV P 4014. †*Rhombopterygia rajoides,* MHMH HDJ 483. †*Shizorhiza stromeri* (Smith et al. 2015, text-fig. 1a-l; 2a-f; NHMUK PV P 73625). †*Sclerorhynchus atavus* (NHMUK PV P4017, 4776, 49546, 49518, 49533, 49547). †*Spathobatis bugesicus* (NHMUK PV P 6010, 2099 (2), BSP AS I 505, BSP 1952 I 82). †*Stahlraja sertanensis,* UERJ-PMB 400, MPSC-P 099; Specimen figured in Brito et al. (2013; text-fig: 3. †*Tethybatis selachoides,* MCSNV 515-516, 511-512. †*Tingitanius tenuimandibulus,* NHMUK PV P66857; Specimen figured in Claeson et al. (2013; text-figs; 2-7). †*Titanonarke molini* MCSNV IG. VR.67290. Specimen figured in Marramà et al. (2018; text-figs: 3A). †*Tlalocbatus applegatei* IGM 5853; Specimen figured in Brito et al. (2019; text-figs: 2-3).

Extant material—*Amblyraja radiata* (BRC-Amblyraja, skeleton). *Aptychotrema vincentian*a (CT-Scan available in https://sharksrays.org). *Glaucostegus typus* (NHMUK

1967.2.11.3, CT-Scan). *Hydrolagus affinis* (BRC-*Hydrolagus*, skeleton). *Chimaera cubana* (CT-Scan available in https://sharksrays.org). *Gymnura altavela* (CT-Scan available in https://sharksrays.org). *Heptranchias perlo* (CT-Scan available in https://sharksrays.org). *Hexanchus nakamurai* (CT-Scan available in https://sharksrays.org). *Hypnos monopterygius* (CT-Scan available in https://sharksrays.org). *Irolita waitil* (CT-Scan available in https://sharksrays.org). *Mobula munkiana* (CT-Scan available in https://sharksrays.org). *Narcine brasiliensis* (CNPE-IBUNAM 9280, skeleton). *Narcine entemedor* (CNPE-IBUNAM 5807, CT-Scan). *Narcine tasmaniensis* (NHMUK 1961, CT-Scan). *Platyrhina* (BRC-*Platyrhina*, CT-Scan). *Platyrhinoidis triseriata* (MNHN 4329, CT-Scan available in https://sharksrays.org). *Pristis* (BRC-*Pristis*, CT scan). *Raja clavata* (BRC-*Raja*, CT-Scan). *Raja eglanteria* (CT-Scan available in https://sharksrays.org). *Rajella fyllale* (BRC-*Rajella*, skeleton). *Rhina ancylostoma* (NHMUK 1884, 1925, CT-Scan). *Rhinobatos glaucostigma* (CNPE-IBUNAM 17810, CT-Scan). *Rhinobatos horkelli* (UERJ 1397, skeleton). *Rhinobatos lentiginosus* (CNPE-IBUNAM 17827, CT-Scan). *Rhinobatos leucorhynchus* (CNPE-IBUNAM 1039, X-ray). *Rhinobatos percellens* (UERJ 1240, skeleton). *Rhinobatos productus* (CNPE-IBUNAM 17829, CT-Scan; 17821 X-ray). *Rhinoptera bonansus* (BRC-*Rhinoptera*, skeleton; CT-Scan available in https://sharksrays.org). *Rhynchobatus djiddensis* (MNHN 7850, X-ray). *Rhynchobatus lübberti* (MNHN 50-22-04.80). *Rhynchobatus sp.* (BCR-*Rhynchobatus*, skeleton). *Tetronarce nobiliana* (CNPE-IBUNAM 9869, CT-Scan). Torpedo (NHMUK 72261). *Trygonorrhina fasciata* (MNHN 1372; BRC-*Trygonorrhina*, CT-Scan). *Urobatis jamaicensis* (AMNH 30385). *Urolophus aurantiacus* (CT-Scan available in https://sharksrays.org). *Urotrygon chilensis* (CT-Scan available in https://sharksrays.org). *Zanobatus sp.* (MNHN 1989.12.91, X-ray; CT-Scan available in https://sharksrays.org). *Zapteryx brevirostris* (UERJ-PMB 35, skeleton; UERJ 1234, 1237, skeleton). *Zapteryx exasperata* (CNPE-

IBUNAM 17822, 17823, 17824, 17826, 17825, 20528, CT- Scan and skeleton). *Zapteryx xyster* (CNPE-IBUNAM 1666, 19790, CT-Scan & skeleton).

Phylogenetic analysis

A matrix of 55 terminals and 95 characters was assembled in Mesquite 3.31 (Maddison & Maddison, 2018) (supplemental material), and analyzed with Mr Bayes (3.2.6) (Ronquist & Huelsenbeck, 2003) in CIPRES (Miller et al., 2010). The matrix included the oldest known skeletal remains or at least a fossil representative of the four classically recognized orders of batoids (Rajiformes, Torpediniformes, Rhinopristiformes, and Myliobatiformes) (Fricke et al., 2019), along with several fossil batoids with unknown phylogenetic affiliations, and the outgroup composed of the Jurassic taxa: †*Belemnobatis,* †*Spathobatis,* †*Kimmerobatis,* and †*Asterodermus.*

Two analyses with the same topological constraints were performed: a non-timescale analysis to produce a phylogeny to be time-scaled using '*a posteriori*' methods, and a tip-dating analysis (supplemental material). In both analyses, strong constraints were used to define the order level clades based on molecular analysis (sensu Naylor et al., 2012). Within these constraints, a large group was included, which contained Rhinopristiformes, Myliobatiformes and several Cretaceous batoids (†'*Rhinobatos' grandis*, †'*R.' latus*, † *'R.' intermedius*, † *'R.' hakelesis*, † *'R.' tenuirostris*, † *'R' marinota*, †*Rhombopterygia*, †*Stahlraja*, and †*Tlalocbatus*). This constraint was used to reduce the comparison available for these fossil taxa and follows previous phylogenetic results (e.g., Claeson et al., 2013; Underwood & Claeson, 2017; Brito et al., 2019). Based on Claeson et al. (2013) and Brito et al. (2013), †*Britobatos*, †*Tethybatis*, †*Tingitanius* were placed in Platyrhinidae. The only un-constrained order was Rajiformes, whose relation to sclerorhynchoids was previously established by Villalobos et al. (2019a).

Parameters for the Bayesian analysis— Datatype: what kind of data is being analyzed (STANDARD = morphological traits). Rates: sets the model for character rate variation (gamma = rates were allowed to vary, permitting the model to estimate evolutionary rates for each character independently from a gamma distribution). Ratepr: this parameter allows the user to specify the rates model between partitions (fixed, as there is only one partition (morphological); there was no need to vary across partitions). Samplefreq: specifies how often the Markov chain is sampled, in this case, 1000. Printfr: how often information about the chain is printed to the screen (1000). Diagnfreq: number of generations between the calculation of MCMC diagnostics (2000). Nruns: determines how many files from independent analyses will be summarized (4). Nchain: establish how many chains are run for each analysis for the MCMCMC (Default setting = 4). Temp: parameter for heating the chains. These parameters facilitate the change of states between the con and heated chains (Dembo *et al.,* 2015 recommendation = 0.2). Relburnin: what proportion of the sampled values will be discarded (Default = yes). Burninfrac: proportion to be discarded (Default = 0.25) savebrlens = yes.

Parameters for the tip-date analysis— prset clockvarp: specify the type of clock the user is assuming (igr, Relaxed clock model where each branch has an independent rate drawn from a gamma distribution). prset brlenspr: this parameter specifies the prior probability distribution on branch lengths. clock: fossilization, we are using data with extant and extinct samples. nodeagepr: specifies the assumptions concerning the age of the terminal and interior nodes in the tree (calibrated, as terminals are not of the same age). igrvarpr: specify a prior on the variance of the gamma distribution from which the branch lengths are drawn in the independent branch rate (IGR) relaxed clock (uniform (0.0001, 200), a vague prior established by Mazke & Wright, (2016) it enforces a relaxed clock for the analysis). prset samplestrat: sets the strategy under which species

were sampled in the analysis (random, default setting assumes extant taxa are sampled randomly while fossils are sampled on constant rates). prset speciationpr: parameter sets the prior on the net speciation rate (uniform (0, 10), default setting value used in Bapst et al., (2016)). prset extinctionpr: this parameter sets the prior on the relative extinction rate (beta (1, 1), flat, extinction is relative to speciation thus between 0 and 1, default settings used in Bapst et al. (2016)). prset fossilizationpr: parameter sets the prior on the relative fossilization rate (beta (1, 1), flat, sampling is psi / (mu + psi), 0 – 1, default setting used in Bapst et al. (2016)). prset clockratepr: parameter specifies the prior assumptions concerning the character change rate of the tree (normal (0.0025, 0.1), vague prior that assumes a flat, Clock Rate Prior used by Mazke & Wright, (2016) and Bapst et al. (2016). It provides little information regarding the character change rate and is used for morphological data in which it is difficult to make assumptions concerning the character change rate.

Indices of stratigraphic congruence for each tree topology were calculated to evaluate the results recovered by the different time-scaling methods, using the R package **strap** (Bell & Lloyd, 2015) and the function **StratPhyloCongruence** (supplemental material). These indices assess different aspects of the relations of a cladogram and the fossil record and should be reported together (e.g., stratigraphic consistency index (SCI), measures the congruence between first appearance date in the fossil record and nodal distances from the root. The relative completeness index (RCI), assess the completeness of the fossil record, whereas the gap excess ratio (GER) and derivatives, compare the extent of ghost ranges implied by the topologies).

None of the indices proposed to date are free of biases and are also affected by different factors (e.g., tree size, percentage resolution, tree shape, the mean age of the tree, range of first

appearances, size of the character matrix). O'Connor & Wills (2016) place tree balance (shape) as one of the main causes affecting the values of stratigraphy indices, and as the different time scaling methods have different approaches towards polytomies (solving them or not) that ultimately can affect tree shape, the Colless' index and the percentage of resolution were estimated to quantify this change. The Colless' index is an estimate of the tree shape; it was calculated using the R package **apTreeshape** (Bortolussi et al., 2005) and the function **colles** (supplemental material), while the percentage of resolved nodes was calculated using O'Connor & Wills (2016) formula.

Time-scaling methods

Two APT ('a *posteriori'* time-scaling) methods were implemented, both of them are available in the R package **Paleotree** (Bapst, 2012) with the **timePaleoPhy** function and specified with the type parameter (supplemental material):

Minimum branch length (MBL) (Laurin, 2004) — scales all branches, so they are greater than or equal to a time variable and subtract time added to later branches from earlier ones to maintain the temporal structure of events.

Basic (Smith, 1994) — is the simplest of time-scaling methods as it ignores time variables, and the nodes are scaled, so they are as old as the first appearance of their oldest descendant (supplemental material).

Tip-dating — Presently, there are no standard methods for tip-dating with morphological data. The selection of parameters was based on Dembo et al. (2015), Matzke & Wright (2016), and Bapst et al. (2016) (supplemental material). Two models of node calibration were used and are available in MrBayes with the commands fixed and uniform. The marginal likelihood of these

two models was used to assess how well they adjust to a given data (Xie et al., 2010). The marginal likelihood was calculated using the steppingstone algorithm implemented in Mr Bayes (Xie et al., 2010). As the uniform command requires an interval of ages a minimum and a maximum, in the cases of extant species with no fossil record, the age of the oldest fossil representative within the clade was used as the maximum limit.

The node ages of the tip dated trees were visualized with FigTree (v.1.4.3) software (available at http://tree.bio.ed.ac.uk/software/figtree). The node ages for the ATP methods were recovered with the **GetNodeAges** function of the R package **claddis** (Lloyd, 2016) (supplemental material).

Stratigraphic Consistency Index (SCI) (Huelsenbeck, 1994) — It assess the congruence between first appearance date in the fossil record and nodal distances from the root. Calculated as the ratio of the number of stratigraphically consistent nodes (i.e., those which terminals are the same age or younger than those of their sister node) to the total of nodes excluding the root. The SCI ranges from 0.0 (maximally inconsistent) to 1.0 (maximally consistent).

Gap Excess Ratio (GER) (Wills, 1999) — Expressed as the Minimum Implied Gap (MIG) scaled between the ghost ranges of the optimal (Gmin) and maximally suboptimal (Gmax) possible topologies. Its values range from 0.0 (maximally suboptimal fit) to 1.0 (optimal fit). However, the GER can never reach the theoretical minimum or maximum on a balanced tree, as the MIG can never be equal to either Gmin or Gmax.

Modified Manhattan Stratigraphic Measure (MSM) (Pol & Norell,2001) — Can be derived from parsimoniously optimizing the first appearance of taxa as an irreversible Sankoff

character on a tree and calculating the total length of the resultant phylogeny. The MSM ranges from 1.0 when the Sankoff character is optimized with the minimum possible steps (best possible fit) and tends towards 0 as the number of steps increases (although a value of zero is never reached).

Relative Completeness Index (RCI) (Benton & Storrs, 1994) —It operates slightly differently from the other indices. Nodes are not simply consistent or inconsistent, but rather contribute to an overall measure of "inconsistency" (the overall ghost range or minimum implied gap MIG) in proportion to the difference between the ages of origin of the branches (or taxa) they support. The MIG is divided by the total observed range length or standard range length (SRL), and the complement of this value expressed as a percentage to yield the RCI. The RCI is not limited to values between 0 and 100, as it can have a negative score if the MIG is greater than the SRL (total observed range).

RESULTS

Phylogenetic analyses

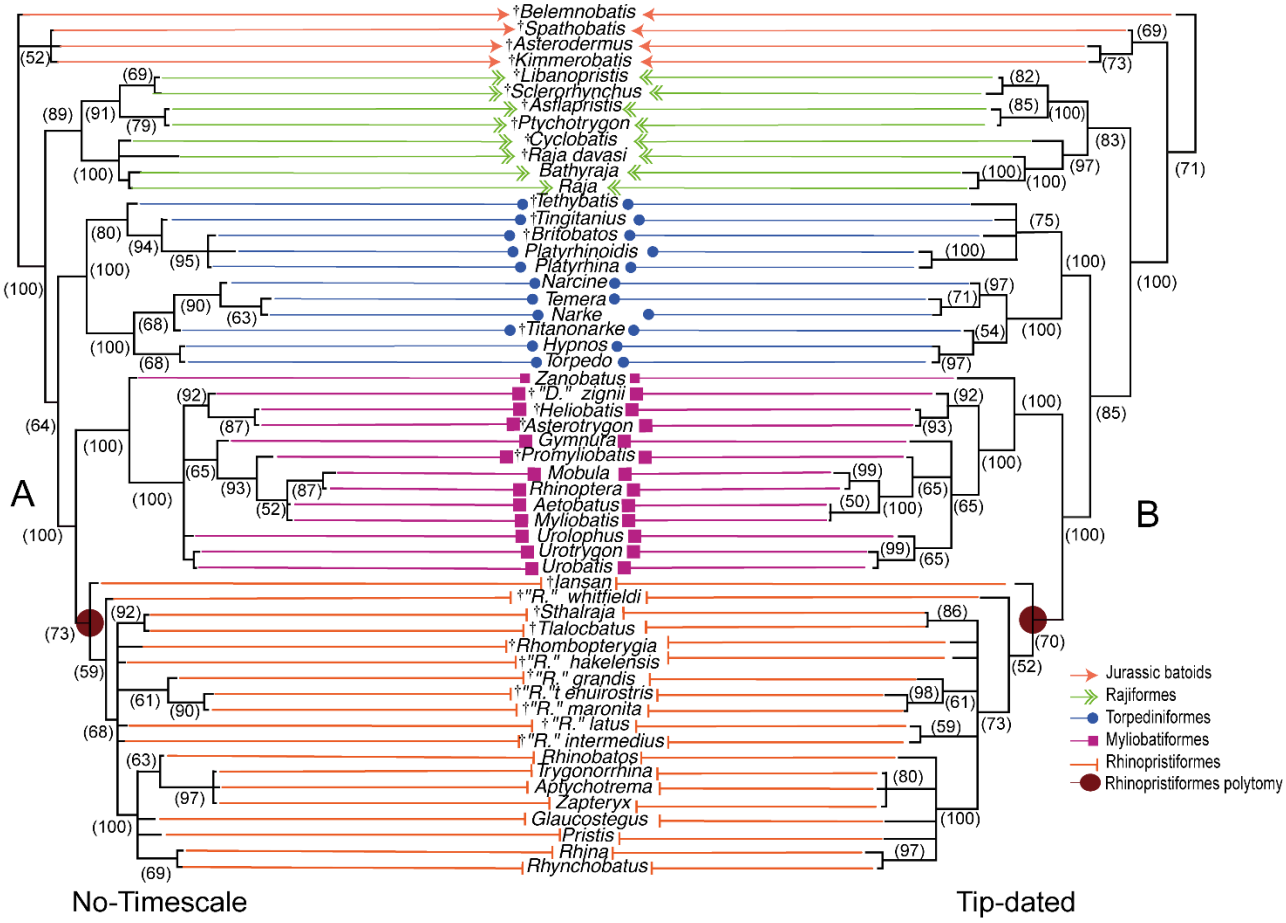

FIGURE 1[size:183mm]. Cladograms resulted from the analyses; clade credibility is placed beneath the clades. **A**. Non-timescaled and **B**. Tip-dating. Orders mark with different shapes. Rhinopristiformes polytomy mark with a dot.

Both analyses (non-timescale and tip-dated) recovered four large monophyletic groups marked with different shapes in Figure 1, which represent the four recognized orders of batoids (Fricke et al., 2019). The arrangement of these orders is similar to that found by molecular analyses (e.g., Douady et al., 2003; Aschliman et al., 2012b; Naylor et al., 2012; Last et al., 2016) (Fig. 1).

A large polytomy characterizes the present topology (marked with a circle, Fig. 1) that includes several Cretaceous batoids (†'*R.' grandis,* †'*R.' latus,* †'*R.' intermedius,* †'*R.' hakelesis*, †'*R.' tenuirostris,* † *'R' marinota,* †*Rhombopterygia*, †*Stahlraja*, and †*Tlalocbatus*) and the Rhinopristiformes (Posterior probability (Pp) = 68%; Fig. 1A, Pp = 73; Fig. 1B). Both analyses failed to recover similar phylogenetic relations to those found by previous analyses for these fossil taxa (Claeson *et al.*, 2013; Georges, 2016; Underwood & Claeson, 2017; Brito *et al.*, 2019) and are placed in close relation to Rhinopristiformes with no further affiliation.

In both analyses, the Jurassic batoids (†*Belemnobatis*, †*Spathobatis*, †*Kimmerobatis*, and †*Asterodermus*) are separated from any member of Rhinopristiformes; this contrasts with previous works (e.g., Claeson et al., 2013; Underwood & Claeson, 2017) and maybe a result of a more inclusive taxon sampling of the present study. The non-timescale analysis placed †*Belemnobatis* at the base of a polytomy within a monophyletic group composed of the remaining Jurassic batoids (Pp =100%; Fig. 1A). While the tip-dated analysis recovered †*Belemnobatis* as the root, separated from the remaining Jurassic taxa (†*Spathobatis*, †*Kimmerobatis*, and †*Asterodermus*) with a posterior probability (Pp) of 71% (Fig. 1B). The remaining Jurassic taxa form a monophyletic group (Pp = 69), in a sister group relation to all remaining batoids (Pp = 100%; Fig. 1B).

Rajiformes (Sclerorhynchoidei + rajoids) is the following group to diverge in both analyses and are placed in a sister group to the remaining batoids (Pp = 89%; Fig. 1A, Pp = 83%; Fig. 1B). Both analyses placed †*Cyclobatis* within Rajiformes, as suggested by Claeson (2010) (Pp = 100% Fig. 1A, Pp = 97%; Fig. 1B). The tip-dated analysis further places †*Raja davisi* as a sister group to the extant rajoids (Pp = 73%; Fig. 1B).

Following the phylogenetic relations proposed by molecular data (e.g., Naylor et al., 2012; Last et al., 2016) and under the uncertainty of morphological data (Aschliman et al., 2012a; Villalobos et al. 2019a), a topological constraint was used for Torpediniformes to include Platyrhinidae. The non-timescale analysis recovered a more resolved topology for the group, with †*Tethybatis* as a sister group for the remaining platyrhinoids (†*Tingitanius,* †*Britobatos, Platyrhina,* and *Platyrhinoidis*) (Pp = 80%; Fig. 1A). Within this clade, †*Tingitanius* is the next taxon to diverge (Pp = 94%; Fig. 1A), followed by a polytomy that includes †*Britobatos* and modern platyrhinoids (Pp = 95%; Fig. 1A). While, the tip-dated analysis recovered a polytomy that includes all fossil taxa along with extant platyrhinoids (Pp = 75%; Fig. 1B). The placement of these fossil taxa within Platyrhinidae follows that of previous phylogenetic analyses (De Carvalho 2006; Claeson et al., 2013; Brito et al., 2013).

Similar topologies were found for the electric rays by both analyses (tip-dated and not-timescale), with the only difference being the placement of †*Titanonarke,* which was placed as a sister taxon to the *Narcine, Narke* and *Temera* clade (Pp = 68%) by the non-timescale analysis and as the sister taxon to the *Hypnos* and *Torpedo* clade (Pp = 54%) by the tip-dated analysis.

Both analyses recovered a similar arrangement for Myliobatiformes to that proposed by molecular analysis (e.g., Aschliman et al., 2012b; Naylor et al., 2012). With the panrays (*Zanobatus*) placed as a sister group for the remaining myliobatoids (Pp = 100%; Fig. 1A-B). The placement of the monophyletic group that includes the fossil myliobatoids (†*Heliobatis*, †*Asterotrygon,* †*'Dasyatis' zignii* and †*Promyliobatis*) varies between analyses (Pp = 92; Fig. 1A-B). The tip-dating analysis recovered a more resolved topology, placing these fossil myliobatoids as a sister group to the remaining Myliobatiformes except for *Zanobatus* (Pp = 100%; Fig. 1B).

Whereas the non-timescale analysis place this latter fossil clade as part of a polytomy (Pp = 100%; Fig. 1A) that includes all of the remaining myliobatoids in a slightly similar position to that recovered by De Carvalho et al. (2004) at least for †*Heliobatis* and †*Asterotrygon* as † *'Dasyatis' zignii* was not included in that study. Within this clade †*Promyliobatis* is recovered in close relation to *Myliobatis*, *Rhinoptera* and *Mobula* (Myliobatinae) (Pp = 93%; Fig. 1A, Pp = 65%; Fig. 1B).

All modern Rhinopristiformes are placed in a polytomy by both analyses, which includes two monophyletic groups: Trygonorrhinidae (Pp = 97; Fig. 1A, Pp = 80; Fig. 1B) and *Rhina+Rhynchobatus* (Pp = 69; Fig. 1A, Pp = 97; Fig. 1B). Both of these clades have also been recovered by molecular data (Aschliman et al., 2012b; Naylor et al., 2012; Last et al., 2016).

Comparison between time-scaled analysis

Stratigraphic indexes were estimated for each scaling method and compared along with their Colless' index and percentage of resolution (Table 1) (O'Connor & Wills, 2016). All trees yield Colless' values lower than 0.5 and a relatively high-resolution percentage, suggesting that in all cases, the topologies are balanced. Probably due to the use of only highly preserved specimens in the analysis.

	SCI	RCI	GER	MSM	Colless' index	% resolution
Tip dating	0.690	66.99	0.91	0.25	0.159	81.13
Basic	0.692	62.25	0.89	0.22	0.150	75.47
MLB	0.692	62.25	0.89	0.22	0.173	75.41

TABLE 1. Stratigraphic indices values, Colless' index and percentage of resolution estimated for the different time scaling methods topologies. **Abbreviations: SCI**, Stratigraphic Consistency Index. **RCI**, Relative Completeness Index. **GER**, Gap Excess Ratio. **MSM**, Modified Manhattan Stratigraphic Measure.

Overall, the GER and MSM values of the tip-dating analysis were better than those of the 'a posteriori' methods, suggesting that its topology implies fewer gaps in the fossil record (Table 1). Because of this, the ages estimated by the tip-dating analysis were used, compared, and discussed against the diversity events proposed by diversity analysis for the neoselachian group (Underwood, 2006; Guinot et al., 2012; Aschliman et al., 2012b).

Node	Tip dating			MLB	Basic	FDA *
	95% L HPD	Mean	95% U HPD			
Jurassic (Root)	157.34	166.04	176.20	178.7	177.7	177.7
Jurassic-Cretaceous + extant batoids between (A)	145.57	159.49	173.60	177.6	175.6	175.6
Rajiformes + remaing batoids (B)	109.93	128.77	147.47	120	113	113
Sclerorhynchoidei - Rajiformes (C)	98.56	115.54	133.78	116	113	113
Ptychotrygonids - sclerorhynchids (D)	79	92.98	106.19	115	113	113
Sclerorhynchoidei - Rajiformes (C)	103.82	121.11	139.45	116	113	113
Ptychotrygonids - sclerorhynchids (D)	94.53	111.48	128.38	115	113	113
Cyclobatoids - Rajoids (F)	85.44	101.54	117.17	100.6	99.6	99.6
Rajoids (E)	67.10	80.16	93.48	71.6	70.6	70.6
Torpediniformes + remaining batoids (G)	99.80	116.82	132.60	120	113	113
Torpediniformes + Platyrhinidae (H)	86.64	106.04	126.61	99	93.9	93.9
Modern electric rays (I)	38.19	52.79	67.46	62.7	58.7	58.7
Rhinopristiformes + Myliobatiformes (J)	97.98	114.26	130.93	118	113	113
Myliobatiformes (K)	61.77	73.53	101.13	70.5	65.5	65.5
Sting rays (L)	46.73	60.79	77.13	69.5	65.5	65.5
Rhinopristiformes (M)	93.92	107.10	120.22	117	113	113
Modern rhinopristoids (N)	32.24	47.86	65.58	58.8	55.8	55.8

TABLE 2**.** Ages of the selected nodes recovered by the different time scaling methods.

Abbreviation: **HPD**, high posterior density interval. **FDA***, first date appearance on the fossil record of the oldest taxon in the clade.

The time-scaling methods used in the present study found differences in the age nodes (Table 2). This variation in the estimated node ages probably reflects discrepancies in the use of the time data (e.g., the tip-dating analysis includes the time data as part of the phylogenetic analysis, leading to slightly different topologies; and in the case of this study a higher resolution percentage, whereas the MLB and basic methods include the age of last and first appearance later not solving polytomies). The use of time data along with the branch length by the tip-dating approach, to evaluate phylogenetic relations might extend back or forward the age of a clade (e.g., the topology recovered in Rajiformes clade by the tip-dating analysis, resulted in pushing further back in time (10 million years (Ma)) the age of this clade (†*Raja davisi* + *Raja* and *Bathyraja*) when compared to the other methods (Table 2).

Tip-dating estimated ages

Two models of node calibration (fixed and uniform), were tested in the tip-dated analysis. The uniform age model recovered a more likely marginal likelihood (-1177.45) compared to the fixed (-1182.44), and therefore, it was the model used.

The uniform model places the divergence time among the Jurassic batoids and the clade leading to Cretaceous + extant batoids between 145.57-173.60 (Ma), with a mean Oxfordian age 159.49 Ma (Table 2, A). Within the Jurassic clade, †*Spathobatis* is recovered as a sister group to

the remaining Jurassic batoids, with a divergence age estimated between 138.43-168.22 Ma and a mean Kimmeridgian age of 153.07 Ma (Table 2).

The divergence between Rajiformes and the remaining batoids occurs between 109.56-147.47 Ma, with a mean Barremian age of 128.77 Ma (Table 2, B). Within this clade, the sclerorhynchoid divergence from the main rajoid clade happened between 98.56-133.75 Ma, with a mean Aptian age of 115.54 Ma (Table 2, C). However, this age was determined using the first and last appearance of †*Libanopristis*, †*Sclerorhynchus*, †*Asflapristis*, and †*Ptychotrygon*, which are not the oldest species for the group. Because of this, a second analysis (supplemental material) was performed using the earliest known record for the Sclerorhynchoidei (†*Onchopristis*, Barremian; Kriwet & Kussius, 2001). This analysis estimated a divergence age for sclerorhynchoid and the main rajoid clade between 103.82-139.45 Ma, with a mean Aptian age of 121.11 Ma (Table 2, C'). In both analyses, the higher limit of the estimated ages places the possible origin of sclerorhynchoids earlier than its oldest known fossil record, within the Valanginian (132.9-139.8 Ma) (Table 2, D'). Within the Sclerorhynchoidei, the divergence of Ptychotrygonidae (sensu Kriwet et al., 2009a) from the remaining sclerorhynchoids is estimated between 79-106.19 Ma with a mean Cenomanian-Turonian age of 92.98 Ma (Table 2, D').

†*Cyclobatis* divergence from the remaining rajoid taxa is calculated between 85.44-117.175 Ma, with a mean Aptian age of 117.17 Ma (Table 2, F). This age suggests that Rajiformes were already a well-establish monophyletic group in the Aptian, with the subsequent divergence of Rajidae between 67.10-93.48 Ma, with a mean Campanian age of 80.16 Ma (Table 2, G).

The separation of Torpediniformes (sensu Naylor et al., 2012 and Last et al., 2016) from the remaining crown batoids (Rhinopristiformes + Myliobatiformes), is estimated between 99.80-

132.60 Ma, with a mean Aptian age of 116.82 Ma (Table 2, G). Inside this group, the divergence between Platyrhinidae and Torpedinoidei + Narcinoidei happened between 86.64-126.61 Ma, with a mean Albian age of 106.04 Ma (Table 2, H), suggesting that both thornback rays and electric rays were already well-defined monophyletic entities in the Albian, followed by the subsequent appearance of extant electric rays between 38.19-67.46 Ma with a mean Ypresian age of 52.79 Ma (Table 2, I).

The separation of Torpediniformes (sensu Naylor et al., 2012 and Last et al., 2016) from the remaining crown batoids (Rhinopristiformes + Myliobatiformes), is estimated between 99.80-132.60 Ma, with a mean Aptian age of 116.82 Ma (Table 2, G). Inside this group, the divergence between Platyrhinidae and Torpedinoidei + Narcinoidei happened between 86.64-126.61 Ma, with a mean Albian age of 106.04 Ma (Table 2, H), suggesting that both thornback rays and electric rays were already well-defined monophyletic entities in the Albian, followed by the subsequent appearance of extant electric rays between 38.19-67.46 Ma with a mean Ypresian age of 52.79 Ma (Table 2, I).

The origin of Rhinopristiformes is calculated between 93.92-120.22 Ma, with a mean Albian age of 107.10 Ma (Table 2, M). With the subsequent divergence of extant (modern) rhinopristoids between 32.24-65.58 Ma, with a mean Ypresian-Lutetian age of 47.86 Ma (Table 2, N).

DISCUSSION

Tip dated analysis

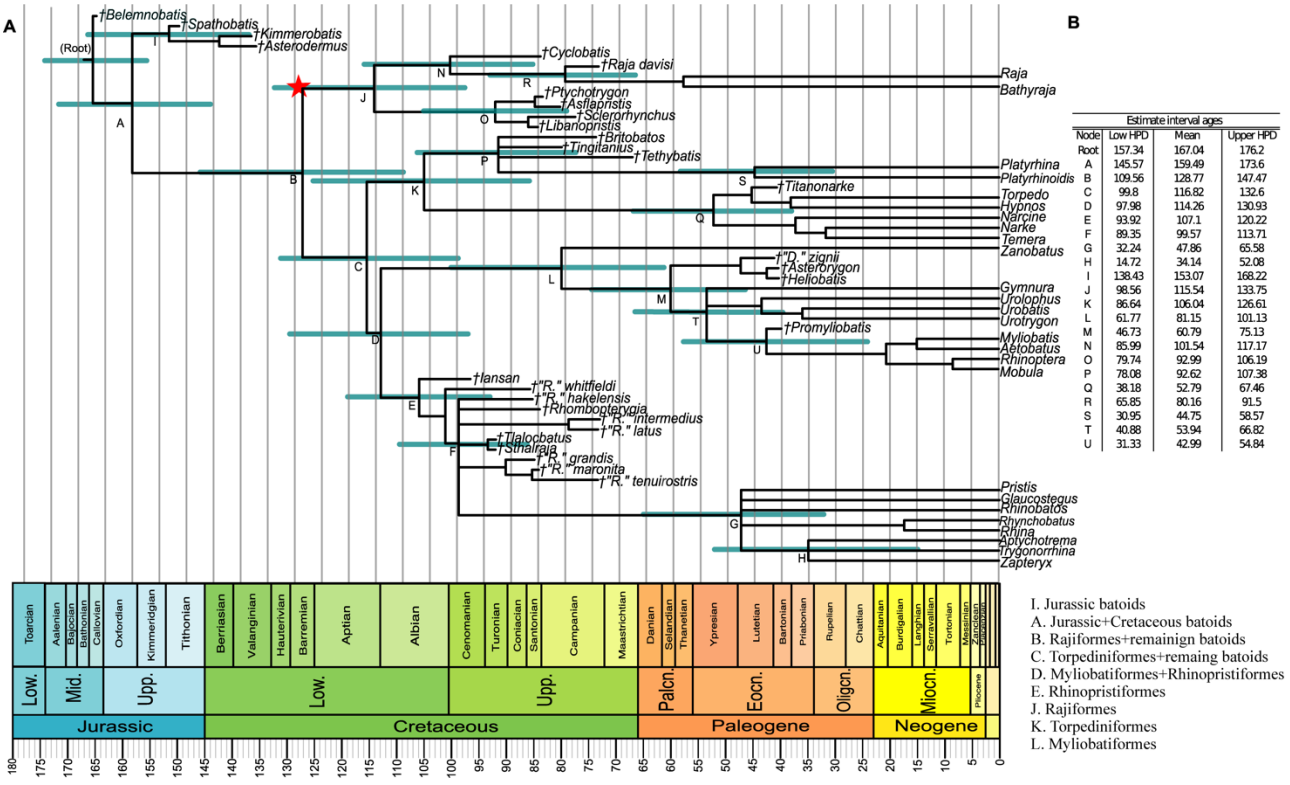

FIGURE 2 [size:183mm]. **A,** Tip-dated tree with estimated divergence ages marked in blue for the relevant clades. Letters refer to the nodes. Age of the oldest fossil record of sclerorhynchoids mark with a star. **B,** High posterior density interval and mean estimated for the nodes marked with letters.

In general, the tip-dating analysis recovered a topology with long internal branches (Fig. 2). This pattern could indicate rapid radiation after an extended period of slow diversification. However, it could also reflect the scarceness of skeletal remains within the fossil record of batoids (Rees, 2002; Underwood & Rees, 2002). The means of the intervals estimated by the present analysis should be considered as a minimum boundary, as the clades recovered were already well-established and differentiated from each other by those times. The upper values of the high posterior density interval (HPD) estimated by the tip-dating are of most interest as, in most cases, extend further back the age of the clades from their known fossil records.

The present analyses (Tip-dating and APT) did not address the possible origin of batoids, as the fossil record from the Late Triassic-Early Jurassic for the group is mostly composed of teeth and therefore was not included in the analysis. However, molecular analyses place the origin of batoids and modern shark groups within the Late Triassic-Early Jurassic (approximately 230 and 200 Ma) (e.g., Delsate & Candoni, 2001; Aschliman et al., 2012b), earlier than the first appearance of any neoselachians belonging to extant clades. Currently, there is no unequivocal batoid remains from the Late Triassic; however, based on histological similarities (lack of a multiple enameloid layers on teeth) it is hypothesized that some neoselachian remains from the Late Triassic (e.g., †*Doratodus* and †*Vallisia*) could be early representatives of batoids (Cuny & Benton, 1999; Botella et al., 2009).

The oldest unambiguous fossil batoid remains come from open marine environments of the Toarcian (Lower Jurassic, approximately 182.7 to 174.1 Ma). A rapid cladogenic episode for neoselachians characterizes this age, probably driven by the colonization of new habitats as a consequence of marine transgression (Underwood, 2006). The fossil remains of this time are mostly fragmentary and dominated by teeth of the genera †*Toarcibatis* and †*Cristabatis* (Cappetta, 2012), with rarer occurrences of the genera †*Belemnobatis* and †*Spathobatis* (Delsate & Candoni, 2001). In the Mid-Late Jurassic (Bathonian to Tithonian) the neoselachian faunas have been described several times (Martill, 1991; Kriwet, 2003; Kriwet & Klug, 2004; Underwood, 2006; Tennant et al., 2017), with batoid diversity dominated by just two genera (†*Spathobatis* and †*Belemnobatis*). This apparent homogenization of batoids diversity is attributed to the reduced diversification and extinction rates of neoselachian product of the absence of barriers in the seas (Kriwet et al., 2009b). However, there seems to be significant sampling bias, as all collected

Jurassic batoid are from near-shore marine sediments and therefore unlikely that represent a full census of the batoids diversity at that time.

The present study included the only four Jurassic genera known from skeletal remains (†*Asterodermus*, †*Belemnobatis*, †*Kimmerobatis*, and †*Spathobatis*). These genera are by no means primitive groups, as they share several synapomorphies with extant species (e.g., synarcual product of the lateral expansion of vertebral arches, presence of antorbital cartilages and aplesodic pectoral fins). Their morphological similarity to the extant taxa, suggests that by the Late-Middle Jurassic batoids were already a well-differentiated monophyletic group. Considering how little their overall morphology has changed since that time, and if a gradual evolutionary scenario is assumed, the morphological evidence also seems to support and even earlier appearance in time, as proposed by the molecular data (Aschliman et al., 2012b).

The estimated age of 145.57-173.60 Ma, for the separation between Jurassic and Cretaceous taxa, is recovered, with a mean Oxfordian age of 159.49 Ma (Fig. 2A). Placing the Jurassic diversification event during an increasingly low sea-level period that reached its lowest stand at the Kimmeridgian-Tithonian boundary, and coincides with the increasing fragmentation of Pangea. These geological events could have impulse diversification events, that would lead to the origination of the Cretaceous groups, by habitat fragmentation of shallow water environments often favoured by batoids.

The placement of Rajiformes as the sister group to the remaining batoids (Fig. 2), is a relationship already established by molecular analyses (e.g., Aschliman et al., 2012b; Naylor et al., 2012; Last et al., 2016). The Rajiformes diversification episode occurred during the Late Jurassic-Early Cretaceous (109.56-147.47 Ma), with a mean Barremian age of 128.77 Ma (Fig.

2B), coinciding with the earliest time from which both Boreal and Tethyan neoselachian faunas are well known, at least in Europe (Underwood, 2006). The Jurassic-Early Cretaceous period presents a combination of short-term catastrophic events, produced from the fragmentation of Pangaea (Scotese, 1991; Nürnberg & Müller, 1991; Monger et al., 1994; Shephard et al., 2013), accompanied by episodes of transgression and regression of the sea level. That led to shifts of circulatory regimes and nutrient flux (Danelian & Kenneth, 2001; Cuny & Benton, 1999), decimating reef environments and leading to dramatic faunal and ecological turnovers between shallow shelf-dwelling faunas and more mobile and ecologically plastic groups.

Prior diversity estimation analyses suggest a steady increase of neoselachian diversity throughout the Late Jurassic-Early Cretaceous, with its lowest point at the J/K (Jurassic-Cretaceous) boundary, associated with a reduced in origination rates and heightened extinction rates (Kriwet & Klug, 2008; Kriwet et al., 2009b), and gradually reaching the diversity peak by the Late Cretaceous (Underwood, 2006; Guinot et al., 2012a). Our results suggest that this increase in diversity may not be as gradual and that Early Cretaceous diversity might be significantly higher, as several divergence events are placed in the Early Cretaceous, suggesting an active cladogenetic period, that led to the Late Cretaceous high diversity.

Within the Rajiformes clade, two monophyletic groups are from (Fig. 2): one that includes all rajoid-like taxa (i.e., †*Cyclobatis*, †*Raja davisi*, *Raja* and *Bathyraja*); and other that contains all sclerorhynchoid taxa. The estimated diverge time between these two clades (98.56 and 133.75 Ma, with a mean Aptian age of 115.54 Ma; Fig 2J), suggest that Rajiformes were already a well-established monophyletic group by the Aptian, with the separation between these two groups as late as the Valanginian (132.9-139.8 Ma). †*Cyclobatis* is a rather peculiar taxon, morphologically

similar to rajoids (e.g., pelvic fin divided into two lobes anterior and posterior) and stingrays (e.g., reduced antorbital cartilages). In the present study, it is placed as the sister group of the remaining rajoids (as suggested by Claeson, 2010), with a divergence time estimated between 85.99-117.17 Ma, with a mean Albian age of 101.54 Ma (Fig. 2N). Within this group, †*Raja davisi* is placed as the sister group to modern rajoids, with a divergence time estimate between 65.85-91.50 M and a mean Campanian age of 80.16 (Fig. 2R) suggesting that Rajidae was already a well-defined monophyletic group in the Campanian, with a divergence time as late as the Early Cenomanian.

The divergence of Torpediniformes + Platyrhinidae from the remaining batoids (Rhinopristiformes and Myliobatiformes) occurred between 99.80-132.60 Ma, with a mean Aptian age of 116.82 Ma (Fig. 2C). These two groups are recovered as one monophyletic group by molecular analysis (e.g., Naylor et al., 2012; Last et al., 2016). Morphologically this classification is problematic, as both groups have very different features. Current fossil evidence does not clarify the relation between these groups, as fossils either present well-defined platyrhinoid features (e.g., †*Tethybatis,* †*Britobatos,* †*Tingitanius*) or torpedinid features (e.g., †*Titanonarke*). Previous morphological analyses that place Platyrhinidae within Myliobatiformes (e.g., McEachran & Aschliman, 2004; Aschliman et al., 2012) are also problematic considering the morphological features between these groups. Perhaps for the moment, the more appropriate approach taxonomically speaking to 'platyrhinoids' is their placement as a family (including all fossil representatives) with uncertain phylogenetic affiliations, as suggested by Claeson (2013) and Villalobos et al. (2019a) analyses. Regardless of our reservations and following the molecular analysis, Torpediniformes + Platyrhinidae were constraint together. As a more detailed analysis and probably further fossil discoveries are needed to assess morphologically, the platyrhinoid placement within Torpediniformes accurately. The divergence age among Torpediniformes and

Platyrhinidae is placed well within the Cretaceous. Estimated as late as the Barremian with a time interval between 86.64-126.61 Ma with a mean Albian age 106.04 Ma (Fig. 2K). The Platyrhinidae (thornback rays) clade includes †*Tethybatis,* †*Britobatos,* and †*Tingitanius,* an association that has been previously suggested by De Carvalho (2004) and Claeson et al. (2013) analyses. With the subsequent divergence of the extant platyrhinoid taxa between 78.08-107.38 Ma, with a mean age of 92.62 Ma (Fig 2P), suggests that Platyrhinidae was a monophyletic group before the Turonian. The Torpedinoidei + Narcinoidei (electric rays) clade includes †*Titanonarke* a relation already established by Claeson (2014) and Marrama et al. (2018).

The separation of Rhinopristiformes and Myliobatiformes is placed in the Cretaceous, occurring as late as the Hauteruvian, with an estimated time of 97.98-130.93 Ma and a mean Aptian age of 114.26 Ma (Fig. 2D). The Rhinopristiformes clade includes several extinct taxa, in a sister group relation to extant rhinopristiforms with †*Iansan* at the base. The estimated divergence time of 89.35-113.71 Ma, with a mean Cenomanian age of 99.5 Ma (Fig. 2F), between extinct (†'*Rhinobatos' grandis,* †'*R.' whitfieldi*, †'*R.' hakelensis,* †'*R.' tenuirostris,* †'*R.' latus,* †'*R.' intermedius* †'*R.' maronita,* † *Rhombopterygia*, †*Tlalocbatus,* and †*Stahlraja*) and extant Rhinopristiformes, suggest that Rhinopristiformes were already a monophyletic group in the Cenomanian, with the earliest divergence time in the Aptian.

The Myliobatiformes clade includes all extinct (†*Heliobatis*, †*Asterotrygon,* † *"Dasyatis" zignii*, and †*Promyliobatis*) and extant stingray taxa. Within this clade, *Zanobatus* placement as a sister taxon to the remaining stingrays is similar to those arrangements of previous morphological analysis (e.g., Aschliman et al., 2012). The ingroup relations of the clade are similar to the molecular hypotheses from Naylor et al. (2012) and Last et al. (2016). The divergence time for the

clade is estimated to be between 61.77-101.13 Ma and a mean of 81.15 Ma (Fig. 2L) and suggest that they were already a well-established monophyletic group in the Campanian, with an earliest estimated divergence time in the Early Cenomanian.

Overall, the present analysis recovered several cladogenetic events during Cretaceous, suggesting a slightly more dynamic increase of diversity for this period. As such, the steady increase of diversity recovered by diversity analyses for this period (Underwood, 2006; Guinot et al., 2012a) might be the product of the transition between a period with a poor fossil record to one with a more complete (e.g., not a single marine neoselachian fauna has been described for the Berriasian, and only three neoselachian species are known from the brackish facies (Underwood 2006)). Current standardization methods cannot adjust time intervals with zero diversity. Therefore, any diversity changes from an unsampled time bin to a sampled one will be an artifact of sampling. Regardless of the cause, all diversity curves studies reviewed suggest that Late Cretaceous standing diversity was substantially higher than that of the Late Jurassic (Underwood, 2006; Kriwet et al., 2009b; Guinot et al., 2012a).

The Cretaceous period presents a substantial rise of global temperature, that caused a reduction of ice in the poles and the spreading of the Atlantic Ocean floor, resulting in a dramatic rise in the sea-level that reached its highest point in the Turonian-Cenomanian (Miller et al., 2005; Tennant et al., 2017). An episodic increase in diversity of marine faunas has been suggested for the Late Cretaceous, and neoselachian diversity seems to follow this pattern (Underwood 2006; Kriwet et al., 2009b; Guinot et al., 2012a). Diversity for the neoselachians was high until the Cenomanian-Turonian anoxic event, which appears as a sudden drop in the number of taxa, followed by a steady recovery through the Coniacian/Santonian, then followed by another decrease

in diversity after the Santonian/Campanian. This low biodiversity level was also found in other marine organism diversity curves (Lloyd et al., 2012), but has not been attributed to a specific geological event. Finally, neoselachian diversity reaches its maximum stance during the Campanian-Maastrichtian (approx. 83.6-66 Ma) (Underwood, 2006; Guinot et al., 2012a).

After the Cretaceous-Paleocene boundary (K/Pg) and through the Paleogene, several divergence events occur, leading to the extant groups of batoids. Within the Torpediniformes + Platyrhinidae clade, the estimated divergence time among *Platyrhina* and *Platyrhinoidis* is between 30.95-58.57 Ma, with a mean Lutetian age of 44.75 Ma (Fig. 2S). The divergence time between extant electric rays and †*Titanonarke* happened between 38.19-67.46 Ma, with a mean Ypresian age of 52.79 Ma (Fig. 2Q). The diverge between †*Heliobatis*, †*Asterotrygon,* †*'Dasyatis' zignii*, and more derived myliobatoids is estimated to be between 46.73-75.13 Ma with a mean of 60.79 Ma (Selandian) (Fig. 2M). All modern genera of Rhinopristiformes also underwent a significant radiation event during the Paleocene, with an estimated divergence time between 32.24-65.58 Ma and a mean Lutetian age of 47.86 Ma (Fig. 2G). Within this clade, the divergence time of Trygonorrhinidae from other extant Rhinopristiformes is estimated between 14.72-52.08 Ma, with a mean Priabonian age of 34.14 Ma (Fig. 2H).

These divergency events coincide with the rapid recovery in neoselachian diversity after the Cretaceous-Paleocene boundary (K/Pg) (Underwood, 2006; Guinot et al., 2012a) and with the global climate changes during the Paleocene, shifting from a warmer earth with high sea levels during the Eocene to a colder climate with glaciation in the Oligocene (Miller et al., 2005). This reduction of Earth's temperature is attributed to continental movement, which resulted in the Northward drift of Australia and India, the opening of the Drake Passage, and the establishment

of the circum-Antarctic current, leading to the thermal isolation of Antarctica (Ehrmann & Mackensen, 1992). These climatic cooling events occurred in a series of threshold events, with transitions between events of rapid cooling that caused a decrease in the sea level and possibly an inverse effect to that of the Cretaceous greenhouse. The cooling of the sea also had an effect in primary production in the seas, causing stress in higher up in the food chain and leading to changes in the diversity (Corliss et al., 1984). These assertions are supported by the present analysis, which places the radiation of all modern batoids clades in the Early-Middle Paleogene period.

CONCLUSION

In general, tip-dating obtained better scores in the stratigraphic indexes than that of the other time scaling methods. This is particularly evident in the case of the GER and MSM indexes, which suggest that the tip-dated topology presents a better fit with the known fossil record, and the implies fewer gaps in the fossil record (Table 1). The tip-dating analysis placed the possible divergence time of the sclerorhynchoid + rajoid clade, between the Valanginian and Cenomanian with a mean in the Aptian. Both the mean and lower limit (Cenomanian) fall within the known fossil record appearances of the group (Table 1). However, the upper limit Valanginian falls well beyond the oldest known record of the group (Barremian, Kriwet et al., 2009a). Considering that this oldest record belongs to †*Onchopristis numidus*, which shares several characteristics with more latter taxa (e.g., †*Ischyrhiza* and †*Schizorhiza*) (Villalobos et al., 2019b), the upper limit of the divergence age estimate may be accurate. The estimated age for the divergence between Ptychotrygonidae (sensu Kriwet et al., 2009a) from other sclerorhynchoids is between 79-106.19 Ma with a mean of 92.98 Ma falling within the oldest period reported for the group (Albian; Kriwet, 1999a; Kriwet et al., 2009a Kriwet & Kussius, 2001).

The present analysis recovered later divergence time intervals than those estimated by the molecular analysis (Aschliman et al., 2012b; text-fig. 4), as expected from previous comparisons among morphological and molecular phylogenies of Neoselachii and the fossil record (Maisey, 2004; Underwood, 2006). The molecular analysis proposes longer evolution times for the batoids as cladogenic episodes are placed earlier in the Early-Middle Jurassic. With subsequent episodes leading to the major groups (Orders; *sensu* Naylor et al., 2012) in the Middle-Late Jurassic. Additional cladogenic events within those groups are proposed in the Late Cretaceous-Early Paleocene, whereas the present analysis places all major divergence events leading to all extant orders of batoids in the Late Jurassic-Early Cretaceous, with subsequent divergences within these clades during the Late Cretaceous and Early-Mid Paleocene. When compared with the fossil record, the estimated ages recovered by the present analysis overlay better with the diversity shifts observed in the fossil record and present a smoother succession of cladogenesis events, with the divergence leading to all extant order of batoids overlaying with the diversity recover after the J/K extinction event, and the diversity rise through the Cretaceous. Molecular divergence age estimates of Middle-Late Jurassic, leading to all extant orders of batoids, contrast with the relative static diversity of neoselachian in that period (Kriwet et al., 2009b).

ACKNOWLEDGMENTS

We thank the NHM for the use of their facilities and equipment for the preparation of the specimens and M. Graham for the training in the use of the equipment. We also thank E. Bernard at the NHMUK for her help with access to and curation of fossil specimens and D.J. Ward for his help and comments. We are particularly indebted to B. Tahiri, M. Ouhouiss, H. and M. Segaoui, who let us purchase the specimens at very reasonable prices and guide us through the localities.

Thanks to the CONACYT for the Ph.D. Scholarship. Also, we would like to thank the two reviewers Kerin Claeson and Todd Cook for and Editors for their time and invaluable contributions to the present work.

LITERATURE CITED

Aschliman, N. C., K. M. Claeson, and J. D. McEachran. 2012a. Phylogeny of Batoidea: pp. 57–95 in J.C. Carrier, J.A. Musick and M.R. Heithaus (eds.). Biology of Sharks and Their Relatives. Second edition. Florida: CRC Press, Boca Raton.

Aschliman, N. C., M. Nishida, M., Miya, J. G., Inoue, K. M., Rosana, and G. J., Naylor. 2012b. Body plan convergence in the evolution of skates and rays (Chondrichthyes: Batoidea). Molecular Phylogenetics and Evolution 63: 28–42.

Bapst, D.W. 2012. Paleotree: an R package for paleontological and phylogenetic analyses of evolution. Methods in Ecology and Evolution 3:803–807.

Bapst DW. 2013. A stochastic rate-calibrated method for time-scaling phylogenies of fossil taxa. Methods in Ecology and Evolution 4:724–733.

Bapst, D.W. and M.J. Hopkins. 2017. Comparing cal3 and other a posteriori time-scaling approaches in a case study with the Pterocephaliid trilobites. Paleobiology 43: 49–67.

Bapst, D. W., A. M., Wright, N. J., Matzke, and G. T., Lloyd. 2016. Topology, divergence dates, and macroevolutionary inferences vary between different tip-dating approaches applied to fossil theropods (Dinosauria). Biology Letters 12: http://dx.doi.org/10.1098/rsbl.2016.0237.

Baum, D. A., and Smith, S. D. 2013. Tree thinking: an introduction to phylogenetic biology. Roberts and Company Publishers, Greenwood Village, 476 pp.

Bell, M. A. and G. T., Lloyd. 2015. strap: an R package for plotting phylogenies against stratigraphy and assessing their stratigraphic congruence. Palaeontology 58:379–389.

Benton, M. J., and P. C. J., Donoghue. 2007. Paleontological Evidence to Date the Tree of Life. Molecular Biology and Evolution. 24: 26–53.

Benton, M. J., and G. W. Storrs. 1994. Testing the quality of the fossil record: paleontological knowledge is improving. Geology. 22:111–114.

Botella, H., P., Plasencia, A., Marquez-Aliaga, G., Cuny, and M., Dorka. 2009. *Pseudodalatias henarejensis* nov. sp. a New Pseudodalatiid (Elasmobranchii) from the Middle Triassic of Spain. Journal of Vertebrate Paleontology 29: 1006–1012.

Bortolussi, N., E., Durand, M., Blum, and O., François, 2005. apTreeshape: Statistical Analysis of Phylogenetic tree shape. Bioinformatics 22:363 –364.

Brito, P., M., Leal, and V. Gallo. 2013. A new lower Cretaceous guitarfish (Chondrichthyes, Batoidea) from the Santana formation, Northeastern Brazil. Boletim do Museu Nacional, Geologia 75:1–13.

Brito, P., E., Villalobos-Segura, and J., Alvarado-Ortega. 2019. A new early cretaceous guitarfish (Chondrichthyes, Batoidea) from the Tlayúa Formation, Puebla, Mexico. Journal of South American Earth Sciences 90:155–161.

Cappetta, H. 2012. Chondrichthyes: Mesozoic and Cenozoic Elasmobranchii: Teeth. Volume 3. Gustav Fischer Verlag. München, 512pp.

Claeson, K., C., Underwood, and D., Ward. 2013. †*Tingitanius tenuimandibulus*, a new platyrhinid batoid from the Turonian (Cretaceous) of Morocco and the Cretaceous radiation of the Platyrhinidae. Journal of Vertebrate Palaeontology 33:1019–1036.

Compagno, L.J. 1977. Phyletic relationships of living sharks and rays. American zoologist 17: 303–322.

Corliss, B. H., M. P., Aubry, W. A., Berggren, J.M., Fenner, L. D., Keigwin, and G., Keller. 1984. The Eocene-Oligocene boundary event in the deep sea. Science 226:806–810.

Cuny, C., and M. J., Benton. 1999. Early radiation of the Neoselachian sharks in Western Europe. (Premiere radiation adaptative des requins néosélaciens en Europe de l'Ouest). GEOBIOS 32:193–204.

Danelian, T., and G. J., Kenneth. 2001. Patterns of biotic change in middle Jurassic to early Cretaceous Tethyan Radiolaria. Marine Micropalentology 43:239–260.

De Carvalho, M. 2004. A Late Cretaceous thornback ray from southern Italy, with a phylogenetic reappraisal of the Platyrhinidae (Chondrichthyes: Batoidea). pp 75–99 in: G., Arriatia, and

A., Tintori (eds.), Mesozoic fishes Systematics Paleoenvironments and Biodiversity, Volume 3, Verlag Dr. Friedrich Pfeil. München.

Delsate, D., and L. W., Candoni, 2001. Description de nouveaux morphotypes dentaires de Batomorphii toarciens (Jurassique inférieur) du Bassin de Paris: Archaeobatidae nov. fam. Bulletin de la Société des naturalistes luxembourgeois 102:131–144.

Douady, C. J., M., Dosay, M. S., Shivji, and M. J., Stanhope. 2003. Molecular phylogenetic evidence refuting the hypothesis of Batoidea (rays and skates) as derived sharks. Molecular phylogenetics and evolution 26: 215–221.

Dunn, K. A., and J. F., Morrissey. 1995. Molecular phylogeny of elasmobranchs Copeia 1995: 526–531.

Ehrmann, W.U., and A., Mackensen.1992. Sedimentological evidence for the formation of an East Antarctic ice sheet in Eocene/Oligocene time. Palaeogeography, Palaeoclimatology, Palaeoecology 93:85–112.

Fricke, R., Eschmeyer, W. N. and Fong, J. D. 2019 Species by Family/Subfamily. Available at http://researcharchive.calacademy.org/research/ichthyology/catalog/SpeciesByFamily.asp 09/Feb/2019

Guinot, G., S., Adnet, and H., Cappetta. 2012. An analytical approach for estimating fossil record and diversification events in sharks, skates and rays. PLoS One. 7(9): https://doi.org/10.1371/journal.pone.0044632.

Huelsenbeck, J.P. 1994. Comparing the stratigraphic record to estimates of phylogeny. Paleobiology 20:470–483.

Kriwet, J. 2003. Neoselachian remains (Chondrichthyes; Elasmobranchii) from the middle Jurassic of SW Germany and NW Poland. Acta Paleontologica Polonica 48: 583–594.

Kriwet, J., and M.J., Benton. 2004. Neoselachian (Chondrichthyes, Elasmobranchii) diversity across the Cretaceous–tertiary boundary. Palaeogeography, Palaeoclimatology, Palaeoecology 214:181–194.

Kriwet, J., W., Kiessling, and S., Klug, 2009b. Diversification trajectories and evolutionary life-history traits in early sharks and batoids. Proceedings of the Royal Society of London B: Biological Sciences 276:945–951.

Kriwet, J., E.V., Nunn, and S., Klug. 2009a. Neoselachians (Chondrichthyes, Elasmobranchii) from the Lower and lower Upper Cretaceous of north-eastern Spain. Zoological Journal of the Linnean Society 155: 316–347.

Kriwet, J., and S., Klug. 2004. Late Jurassic selachians (Chondrichthyes, Elasmobranchii) from Southern Germany: Re-evaluation on taxonomy and diversity. Zitteliana 44: 67–95.

Kriwet, J. and S., Klug. 2008. Diversity and biogeography patterns of Late Jurassic Neoselachians (Chondrichthyes: Elasmobranchii). Geological Society, London, Special Publications 295:55–70.

Kriwet, J., and K., Kussius. 2001. Paleobiology and paleobiogeography of sclerorhynchid sawfishes (Chondrichthyes: Batomorphii). Revista Española de Paleontología 16:35– 46.

Last, P., G., Naylor, S., Bernard, W., White, M. R., De Carvalho, and M., Stehmann. 2016. Rays of the World. Csiro Publishing, Australia, 790 pp.

Laurin, M. 2004. The evolution of body size, Cope's Rule and the origin of amniotes. Systematic Biology 53:594–622.

Lloyd, G. T. 2016. Estimating morphological diversity and tempo with discrete character-taxon matrices: implementation, challenges, progress, and future directions. Biological Journal of the Linnean Society. 118: 131–151.

Lloyd, G. T., D. W., Bapst, M., Friedman, and K. E., Davis. 2016. Probabilistic divergence time estimation without branch lengths: dating the origins of dinosaurs, avian flight and crown birds. Biology Letters 12: http://dx.doi.org/10.1098/rsbl.2016.0609

Lloyd, G. T., P. N., Pearson, J. R., Young, and A. B., Smith, 2012. Sampling bias and the fossil record of planktonic foraminifera on land and in the deep sea. Paleobiology 38:569–584.

Maddison, W. P., and D. R., Maddison. 2018. Mesquite: A Modular System for Evolutionary Analysis. Version 3.51 Available at http://mesquiteproject.org.

Marramà, G., G., Carnevale, A., Engelbrecht, K., Claeson, R., Zorzin, M., Fornasiero, and J., Kriwet. 2018. A synoptic review of the Eocene (Ypresian) cartilaginous fishes

(Chondrichthyes: Holocephali, Elasmobranchii) of the Bolca konservat lagerstätte, Italy. Paläontologische Zeitschrift 92:283–313.

Martill, D. M. 1991. Fish: pp 197–225 in D.M., Martill and J. D., Hudson (Eds.). Fossils of the Oxford Clay. Field guides to fossils, Volume 4. Palaeontological Association, London.

Matzke, N. J., and A., Wright. 2016. Inferring node dates from tip dates in fossil Canidae: the importance of tree priors. Biology letters 12: https://doi.org/10.1098/rsbl.2016.0328.

Miller, K. G., M. A., Kominz, J. V., Browning, J. D., Wright, G. S., Mountain, M. E., Katz, P. J., Sugarman, B. S., Cramer, N., Christie-Blick, and S. F., Pekar. 2005. The Phanerozoic record of global sea–level change. Science 310:1293–1298.

Miller, M. A., W., Pfeiffer, and T., Schwartz. 2010. Creating the CIPRES Science Gateway for inference of large phylogenetic trees. in Proceedings of the Gateway Computing Environments Workshop (GCE), 14 Nov. 2010, New Orleans, LA.1;8

Monger, J. W. H., P., Heyden, M. J., Journeay, C. A., Evenchick, and J. B., Mahoney. 1994. Jurassic-Cretaceous basins along the Canadian coast belt: Their bearing on premid-Cretaceous sinistral displacements. Geology 22:175–178.

Naylor, G. J., J.N., Caira, K., Jensen, K.A., Rosana, N., Straube, and C., Lakner. 2012. Elasmobranch phylogeny: A mitochondrial estimate based on 595 species. pp. 31-56 in J. C., Carrier, J. A., Musick, and M. R., Heithaus, (eds.). Biology of Sharks and Their Relatives. Second edition. Florida: CRC Press, Boca Raton.

Nürnberg, D. and B. Müller. 1991. The tectonic evolution of the South Atlantic from Late Jurassic to present. Tectonophysics 191: 27–53.

O'Connor, A., and M. A., Wills. 2016 Measuring stratigraphic congruence across trees, higher taxa, and time. Systematic biology 65:792–811.

Pol, D. and N. A., Norell. 2001. Comments on the Manhattan stratigraphic measure. Cladistics 17:285–289.

Rees, J. 2002. Shark fauna and depositional environment of the earliest Cretaceous Vitabäck Clays at Eriksdal, southern Sweden. Transactions of the Royal Society of Edinburgh (Earth Sciences) 93:59–71.

Rees, J. 2005. Neoselachain shark and ray teeth from the Valanginian, Lower Cretaceous of Wawal, Central Poland. Palaeontology 48:209–221.

Ronquist, F., and J. P., Huelsenbeck. 2003. Mrbayes 3: Bayesian phylogenetic inference under mixed models. Bioinformatics 19: 1572–1574.

Sansom, R. S., P. G., Choate, J. N., Keating, and E., Randle. 2018. Parsimony, not Bayesian analysis, recovers more stratigraphically congruent phylogenetic trees. Biology letters. 14: https://doi.org/10.1098/rsbl.2018.0263

Schwartz, F. J. and M. B., Maddock. 2002. Cytogenetics of the elasmobranchs: genome evolution and phylogenetic implications. Marine and freshwater research 53: 491–502.

Scotese, R. C. 1991. Jurassic and Cretaceous plate tectonic reconstructions. Paleogeography, Paleoclimatology, Paleoecology 87:493–501.

Siddall, M. E. 1996. Stratigraphic consistency and the shape of things. Systematic Biology 45:111–115.

Siddall, M. E. 1998. Stratigraphic fit to phylogenies: a proposed solution. Cladistics 14:201–208.

Smith, M. M., A., Riley, G. J., Fraser, C., Underwood, M., Welten, J., Kriwet, C., Pfaff, and Z., Johanson. 2015. Early development of rostrum saw-teeth in a fossil ray tests classical theory of the evolution of vertebrate dentitions. Proceedings of the Royal Society B: Biological Sciences 282: https://doi.org/10.1098/rspb.2015.1628.

Stadler, T. 2010. Sampling-through-time in birth–death trees. Journal of theoretical biology 267: 396–404.

Stadler, T., and Z., Yang, 2013. Dating phylogenies with sequentially sampled tips. Systematic biology.62: 674–688.

Shephard, G. E., D. R., Müller, and M., Seton. 2013. The tectonic evolution of the Arctic since Pangea breakup: Integrating constraints from surface geology and geophysics with mantle structure. Earth-Science Reviews 124:148–183.

Tennant, J. P., P. D., Mannion, P., Upchurch, M. D. Sutton and G. D., Price. 2017. Biotic and environmental dynamics through the Late Jurassic-Early Cretaceous transition: evidence for protracted faunal and ecological turnover. Biological Reviews 92:776–814.

Underwood, C. 2006. Diversification of the Neoselachii (Chondrichthyes) during the Jurassic and Cretaceous. Paleobiology 32:215–235.

Underwood, C., and K., Claeson. 2017. The late Jurassic ray *Kimmerobatis etchesi* gen. et sp. nov. and the Jurassic radiation of the Batoidea. Proceedings of the Geologists Association. http://dx.doi.org/10.1016/j.pgeola.2017.06.009

Underwood, C., and J., Rees. 2002. Selachian faunas from the earliest Cretaceous Purbeck Group of Dorset, southern England. Special Papers in Palaeontology 68:83–102.

Villalobos-Segura, E., C. J, Underwood, D. J., Ward, and K. M., Claeson. 2019a. The first three-dimensional fossils of Cretaceous sclerorhynchid sawfish: *Asflapristis cristadentis* gen. et sp. nov., and implications for the phylogenetic relations of the Sclerorhynchoidei (Chondrichthyes). Journal of Systematic Palaeontology. https://doi.org/10.1080/14772019.2019.1578832

Villalobos-Segura, E., C. J. and Ward, D. J. 2019b. In press. The first skeletal record of the Cretaceous enigmatic sawfish genus *Ptychotrygon* (Chondrichthyes: Batoidea) from the Turonian (Cretaceous) of Morocco. Papers in Palaeontology.

Wills, M.A. 1999. Congruence between phylogeny and stratigraphy: randomization tests and the gap excess ratio. Systematic Biology. 48: 559–580.

Winchell, C.J., A.P., Martin, and J., Mallatt. 2004. Phylogeny of elasmobranchs based on LSU and SSU ribosomal RNA genes. Molecular phylogenetics and evolution 31: 214–224.

Xie, W., P. O., Lewis, Y., Fan, L., Kuo, and M. H., Chen. 2010. Improving marginal likelihood estimation for Bayesian phylogenetic model selection. Systematic biology 60:150–160.

Submitted August 23, 2019; revisions (R1) received January 14, 2020; revisions (R2) received March 29, 2020; revision (R3) May 28, 2020; accepted May 29, 2020.